Impact of variable fluid properties on forced convection of Fe_3O_4-CNT/water hybrid nanofluid in a double-pipe mini-channel heat exchanger

Amin Shahsavar[1], Ali Godini[1], Pouyan Talebizadeh Sardari[2], Davood Toghraie[3,*]

[1] Department of Mechanical Engineering, Kermanshah University of Technology, Kermanshah, Iran

[2] Fluids and Thermal Engineering Research Group, Faculty of Engineering, The University of Nottingham, University park, Nottingham, United Kingdom

[3] Department of Mechanical Engineering, Khomeinishahr Branch, Islamic Azad University, Isfahan, Iran

Abstract

The objective of this study is to assess the hydrothermal performance of a non-Newtonian hybrid nanofluid with temperature-dependent thermal conductivity and viscosity compared with a Newtonian hybrid nanofluid with constant thermophysical properties. A counter-current double-pipe mini-channel heat exchanger is studied to analyze the effects of hybrid nanofluid. The nanofluid is employed as the coolant in the tube side while the hot water flows in the annulus side. Two different nanoparticles including Tetra Methyl Ammonium Hydroxide (TMAH) coated Fe_3O_4 (magnetite) nanoparticles and Gum Arabic (GA) coated Carbon Nanotubes (CNTs) are used to prepare the water based hybrid nanofluid. The results demonstrated that the non-Newtonian hybrid nanofluid always has a higher heat transfer rate, overall heat transfer coefficient, effectiveness, and performance index than those of the Newtonian hybrid nanofluid, while the opposite is true for pressure drop and pumping power. Supposing that the Fe_3O_4-CNT/water hybrid nanofluid is a Newtonian fluid with constant thermal conductivity and viscosity, leads to a large error in the

[*]Corresponding author
E-mail address: toghraee@iaukhsh.ac.ir

computation of pressure drop (1.5-9.71%), pumping power (1.5-9.71%), and performance index of heat exchanger (1.86-11.25%), whereas the errors in the computation of heat transfer rate, overall heat transfer coefficient, and effectiveness aren't considerable (less than 2.91%).

Keywords: non-Newtonian hybrid nanofluid; Double-pipe heat exchanger; Magnetite; Carbon nanotube; convective heat transfer

1. Introduction

Double-pipe heat exchangers have been widely employed in various applications to exchange heat between two fluids called as heat transfer fluids [1, 2]. They are an essential part of almost all the industries, including the oil and gas industry, power generation, refrigeration, and nuclear power. Due to the great importance of heat exchangers, improving their efficiency is a very important issue. So far, several methods have been proposed in the literature to enhance heat exchanger performance such as using various fins and turbulators. However, these modifications offer several disadvantages like increase in pressure drop, weight and volume of heat exchangers that limit their usage.

Over the past decade, scientists and researchers around the world have revealed that the heat exchanger performance can be considerably enhanced by improving the thermal conductivity of working fluids [3, 4]. This goal can be achieved through the use of nanofluids, which are prepared by suspending nanoparticles with sizes typically of 1-100 nm in conventional heat transfer fluids such as water, oil, and ethylene glycol [5-8]. This term was first suggested by Choi [9] in 1995, and it has since gained in popularity [10-17].

A great number of experimental and numerical works have been performed on the various aspects of different nanofluids performance in double-pipe heat exchangers [18-22]. Maddah et al. [23] experimentally evaluated the effects of Al_2O_3-water nanofluid on the performance of a horizontal double-pipe heat exchanger under turbulent flow regime and showed 52% and 12% enhancements in the friction factor and heat transfer rate, respectively. Mousavi et al. [24] numerically studied the effect of a variable magnetic field on the hydrothermal characteristics of Fe_3O_4-water nanofluid flowing through a sinusoidal double-pipe heat exchanger and reported the enhancement of Nusselt number in the presence of magnetic field. Saeedan et al. [25] numerically examined the effect of Cu-water, CuO-water and CNT-water nanofluids on the performance of a finned type heat exchanger. They found that both the Nusselt number and pressure drop intensify with increasing nanoparticle concentration. Sarafraz et al. [26] experimentally studied the use of CNT-water nanofluid inside a double-pipe heat exchanger. They assessed the impact of different effective parameters on the convective heat transfer coefficient in laminar and turbulent flow regimes and found that the proposed nanofluid can enhance the heat transfer by almost 44% compared with the pure water. Kumar et al. [27] experimentally surveyed the effect of Fe_3O_4-water nanofluid on the performance of a double pipe heat exchanger with a longitudinal fin with return band under turbulent flow regime. They showed the enhancement of Nusselt number with increasing the Reynolds number and nanoparticle concentration. Hussein [28] experimentally examined the flow of Aluminum Nitride- ethylene glycol nanofluid through a double-pipe heat exchanger and showed the increase of Nusselt number with increasing the flow rate and volume concentration of nanofluid. Shirvan et al. [29] studied the influence of Reynolds number and nanoparticle concentration on the performance of Al_2O_3-water nanofluid inside a double-pipe heat exchanger and showed the enhancement of Nusselt number with increasing the Reynolds number and decreasing the nanoparticle concentration.

To enhance the rate of heat transfer, hybrid nanofluids has attracted lots of attention using a combination of different nanoparticles in the nanofluids in order to take the advantage of them [30-36]. Esfe et al. [37] experimentally studied the thermal conductivity of ethylene glycol based hybrid nanofluid containing ZnO-CNT nanoparticles. They showed the improvement of thermal conductivity using ZnO and CNT nanoparticles compared with the base fluid and developed a new correlation for the calculation of thermal conductivity based on the experimental data using an artificial neural network (ANN).

The combination of Fe_3O_4 with CNT nanoparticles is widely used as a promising hybrid nanofluid. Baby and Sundara [38] studied the effects of nanoparticles concentration on the thermal conductivity of Fe_3O_4-CNT/water hybrid nanofluid and reported 6.5-10% improvement in the thermal conductivity of nanofluid in the temperature range of 30-50 °C compared with the base fluid. Felicia and Philip [39] investigated an oil-based Fe_3O_4-CNT hybrid nanofluid in the presence of a magnetic field and showed the enhancement of viscosity with increasing magnetic field intensity. Sundar et al. [40] experimentally assessed the hydrothermal characteristics of Fe_3O_4-CNT/water hybrid nanofluid in a circular tube and presented 14.8% improvement in the Nusselt number using nanofluid with concentration of 0.3% at Reynolds number of 3000. Shahsavar et al. [41] studied the use of Fe_3O_4-CNT/water hybrid nanofluid in a heated tube in the presence of both constant and alternating magnetic fields. They showed higher improvement of heat transfer using a constant magnetic field compared with an alternating one. Harandi et al. [42] conducted experiments to determine the thermal conductivity of Fe_3O_4-CNT/EG hybrid nanofluid at different temperatures and found the improvement of thermal conductivity with increase in temperature and nanoparticle concentration.

In most of the previous research works on the performance of heat exchangers containing various nanofluids, the thermophysical properties of the nanofluid have been assumed as constant and the nanofluid itself has been considered as Newtonian [43, 44]; while various studies have shown that the thermophysical properties of nanofluids are a function of temperature, and that the majority of nanofluids exhibit a non-Newtonian behavior [45-47]. In this research, we want to see if a significant difference is observed in the performance parameters of a heat exchanger (i.e. pumping power, effectiveness, and performance index) by assuming constant properties and a Newtonian nature for nanofluids. We also want to find out: under what conditions the assumptions of constant properties and Newtonian nature of nanofluid can be used in the analysis of heat exchangers? This is done by comparing the performance parameters of a counter-current double-pipe heat exchanger containing Newtonian Fe_3O_4-CNT/water nanofluid of constant properties with the performance parameters of a heat exchanger containing the non-Newtonian Fe_3O_4-CNT/water hybrid nanofluid with temperature dependent thermal conductivity and viscosity, at different Reynolds numbers and concentrations.

2. Physical properties of nanofluid

This investigation is conducted on a hybrid nanofluid consisting of TMAH coated magnetite nanoparticles and GA coated CNTs. It was prepared by mixing different volume ratios of Fe_3O_4-water nanofluid and CNT-water nanofluid, followed by 5 min sonication [48]. The detailed description of the preparation method can be found in Refs. [48-50]. The magnetite and CNT nanoparticles are attached physically because of interaction between the molecules of TMAH and GA.

After careful preparation and characterization, a series of experiments were performed to evaluate the thermophysical properties of the hybrid nanofluid. The hybrid nanofluid shows the non-Newtonian and Newtonian behaviors at low (up to 70 s^{-1}) and high shear rates, respectively. Additionally, the viscosity of the hybrid nanofluid enhances with increase in volume concentration of nanoparticles, while reduces with increasing the temperature. However, the thermal conductivity increases with temperature and volume concentration.

Based on the data obtained from experiments, the artificial neural network (ANN) was used to find a correlation between the thermal conductivity and temperature and volume concentration of Fe_3O_4 and CNT nanoparticles [51]. For the viscosity, a correlation is developed as a function of temperature, shear rate, and volume concentrations of Fe_3O_4 and CNT nanoparticles [51]. The acquired neural network models illustrate a good accuracy to predict the thermal conductivity and viscosity according to Fig. 1. The correlations developed are presented in appendix A, and it is clear that the models are temperate dependent.

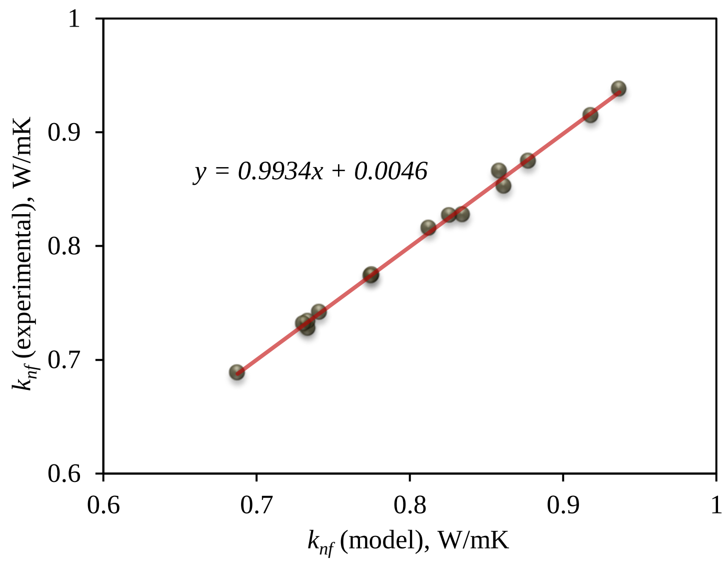

(a)

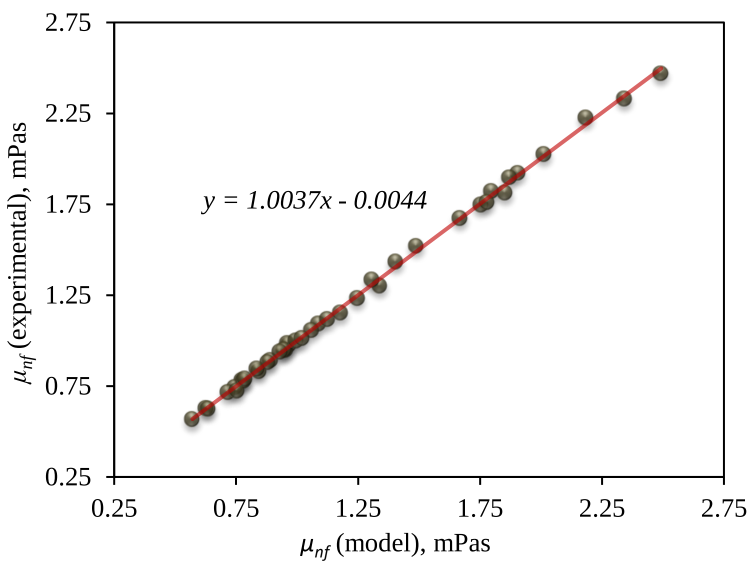

(b)

Fig. 1. Results obtained from the developed models in comparison with the experimental data: (a) thermal conductivity, (b) viscosity [18].

The viscosity and thermal conductivity of the considered Newtonian hybrid nanofluids are reported in Table 1. The considered viscosity for the Newtonian nanofluid is equal to the viscosity of the non-Newtonian nanofluid at the same concentrations of CNT and magnetite nanoparticles at shear rates higher than 70 s^{-1}. Also, the considered thermal conductivity for the Newtonian nanofluid samples is the same as the thermal conductivity of the non-Newtonian nanofluid at the inlet temperature of nanofluid.

Table 1. Characteristics of the studied Newtonian nanofluid samples.

	φ_{CNT} (%) = 0.1%					φ_{CNT} (%) = 1.35%				
	φ_{CNT} (%)					φ_{CNT} (%)				
	0.1	0.3	0.5	0.7	0.9	0.1	0.3	0.5	0.7	0.9
$\mu_{nf} \times 10^4$ (kg/ms)	8.15	9.48	11.08	12.81	14.48	11.33	13.03	14.61	15.95	17.01
k_{nf} (W/mK)	0.691	0.725	0.739	0.759	0.794	0.703	0.759	0.772	0.866	0.902

Moreover, the nanofluid bulk density (ρ_{nf}) and specific heat ($c_{p,nf}$) are computed as:

$$\rho_{nf} = \varphi_M \rho_M + \varphi_{CNT} \rho_{CNT} + (1 - \varphi_M - \varphi_{CNT}) \rho_w \quad (1)$$

$$c_{p,nf} = \varphi_M c_{p,M} + \varphi_{CNT} c_{p,CNT} + (1 - \varphi_M - \varphi_{CNT}) c_{p,w} \quad (2)$$

where φ is the volume concentration of nanoparticles and, subscripts *M*, *CNT* and *w* refer to magnetite, CNT and water, respectively.

3. Mathematical modelling

Due to the small size of nanofluids, they can thus be approximately evaluated as a pure fluid considering no velocity slip and local thermal equilibrium between the base fluid and nanoparticles. The governing equations for laminar, steady state forced convection flow of the studied nanofluid are given as follows:

Continuity:

$$\nabla.\left(\rho_{nf}\boldsymbol{V}\right) = 0 \tag{3}$$

Momentum:

$$\nabla.\left(\rho_{nf}\boldsymbol{V}\boldsymbol{V}\right) = -\nabla p + \nabla.\left(\mu_{nf}\nabla\boldsymbol{V}\right) \tag{4}$$

Energy:

$$\nabla.\left(\rho\boldsymbol{V}c_{p,nf}T\right) = \nabla.\left(k_{nf}\nabla T\right) \tag{5}$$

where $\boldsymbol{V}$ is the velocity, p is the pressure, and T is the temperature.

Reynolds number for the flow of nanofluid (Re_{nf}) and water (Re_w) through the tube side and annulus side, respectively, can be calculated as:

$$Re_{nf} = \frac{\rho_{nf}u_{in,nf}(2r_i)}{\mu_{nf}} \tag{6}$$

$$Re_w = \frac{\rho_w u_{in,w}[2(r_o - r_i)]}{\mu_w} \tag{7}$$

where $u_{in,nf}$ and $u_{in,w}$ are the inlet velocity of the nanofluid and water, respectively.

Considering the fact that the outer wall of the heat exchanger is adiabatic and the problem under consideration is steady state, the rate of heat transfer to the nanofluid from the hot water is equal to that of the hot water according to the conservation of energy ($\dot{Q}_{nf} = \dot{Q}_w = \dot{Q}$) which are obtained as:

$$\dot{Q}_{nf} = \dot{m}_{nf}c_{p,nf}(T_{out} - T_{in})_{nf} \tag{8}$$

$$\dot{Q}_w = \dot{m}_w c_{p,w}(T_{in} - T_{out})_w \tag{9}$$

where $\dot{m}_{nf}$ and $\dot{m}_w$ are mass flow rate of the cold nanofluid and the hot water, respectively.

The overall heat transfer coefficient is given as:

$$U = \frac{\dot{Q}}{A\Delta T_{LMTD}} \tag{10}$$

where A is the internal tube area, and ΔT_{LMTD} is the logarithmic mean temperature difference computed as:

$$\Delta T_{LMTD} = \frac{\Delta T_2 - \Delta T_1}{\ln(\Delta T_2/\Delta T_1)} \tag{11}$$

where $\Delta T_1 = T_{in,w} - T_{out,nf}$ and $\Delta T_2 = T_{out,w} - T_{in,nf}$.

One way of measuring the performance of a heat exchanger is to compute its effectiveness. The heat exchanger effectiveness is ratio of the actual heat transfer rate to the maximum possible one given as:

$$\varepsilon = \frac{\dot{Q}}{\dot{Q}_{max}} = \frac{\dot{Q}}{C_{min}\left(T_{in,w} - T_{in,nf}\right)} \tag{12}$$

where C_{min} represents the minimum heat capacity rate given as:

$$C_{min} = \min\left[C_w, C_{nf}\right] \tag{13}$$

Here, C_w and C_{nf} are respectively heat capacity rates of the water and the nanofluid defined as:

$$C_w = \dot{m}_w c_{p,w} \tag{14}$$

$$C_{nf} = \dot{m}_{nf} c_{p,nf} \tag{15}$$

The minimum heat capacity rate is obtained for the nanofluid and hence, the effectiveness is calculated as:

$$\varepsilon = \frac{T_{out,nf} - T_{in,nf}}{T_{in,w} - T_{in,nf}} \tag{16}$$

The rate of energy consumption required to pump the nanofluid in the heat exchanger is given as:

$$\dot{W} = \dot{V}\Delta p \tag{17}$$

where $\dot{V}$ and Δp denote volumetric flow rate and pressure drop, respectively.

To evaluate the heat transfer rate and the pumping power simultaneously, a parameter called performance index is defined as the ratio of heat transfer rate to the pressure drop given as [52]:

$$\eta = \frac{\dot{Q}}{\Delta p} \tag{18}$$

4. Numerical method and validation

ANSYS-FLUENT software is used to solve the governing equations employing the SIMPLE method for pressure and velocity coupling. The second order upwind method is used to discretize the convective and diffusion terms using the finite-volume method. The convergence criteria is also set to 10^{-6}. A structured quad based mesh was used throughout the domain with a more grid density near the wall. The grid independence study was carried out by considering the numerical results of six different grid resolutions. The results of this investigation is summarized in Table 2. It should be noted that the grid resolution was reported as number of longitudinal nodes×number of radial nodes in central tube×number of radial nodes in annulus. So, by comparing the results, the grid with resolution of 1000×35×35 was chosen. To verify the present numerical procedure, the results are compared with the experimental data of Duangthongsuk and Wongwises [53] for water-TiO_2 nanofluid in a double-pipe heat exchanger shown in Fig. 2. Good agreement between the present results and Ref. [53] is shown with the maximum error of about 5%.

Table 2. Grid independence study for non-Newtonian Fe_3O_4-CNT/water hybrid nanofluid at $\varphi_M = 0.9\%$, $\varphi_{CNT} = 1.35\%$ and $Re = 2000$.

Grid	$\dot{Q}$ (W)	Percentage difference	ΔP(Pa)	Percentage difference
800×25×25	33.92		120.1	
900×30×30	35.82	5.6	125.5	4.5
950×30×30	37.06	3.5	129.1	2.9

1000×30×30	37.92	2.3	132.1	2.3
1000×35×35	**38.23**	**0.8**	**133.7**	**1.2**
1100×35×35	38.51	0.7	134.6	0.67

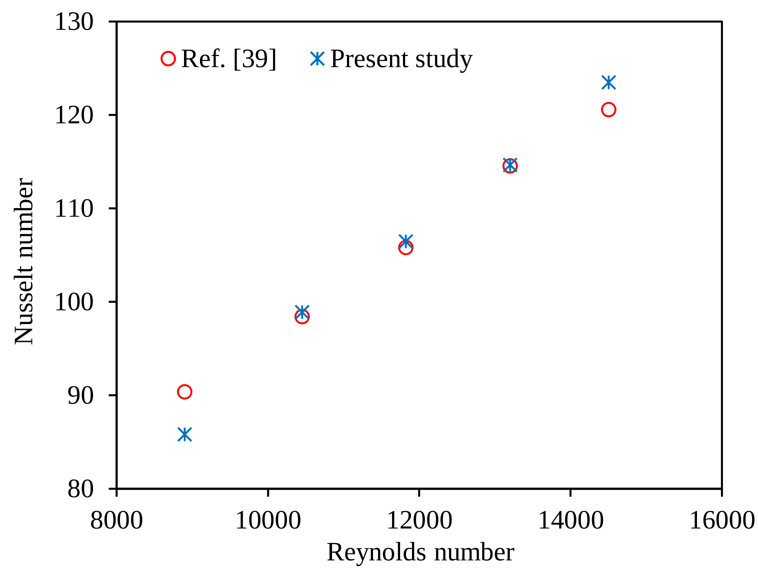

Fig. 2. Comparison between results obtained from present study and experimental results of Ref. [53].

5. Geometry and boundary conditions

The present investigation is conducted in a double-pipe counter-current mini-channel heat exchanger with the length of 1 m, inner diameter of 1 mm, and outer diameter of 2 mm. The thickness of the inner tube's wall is neglected. Fig. 3 illustrates the schematic of the geometry including the flow directions of both hot water and cold nanofluid. Due to the axisymmetric nature of the problem, only half of the geometry is considered as the computational 2-D domain. For the outer wall, adiabatic boundary condition is used. Uniform velocity and uniform temperature are also considered at both tube and annulus entrances while zero relative pressure is utilized at the outlets. Additionally, the no-slip condition is employed on the inner and outer walls.

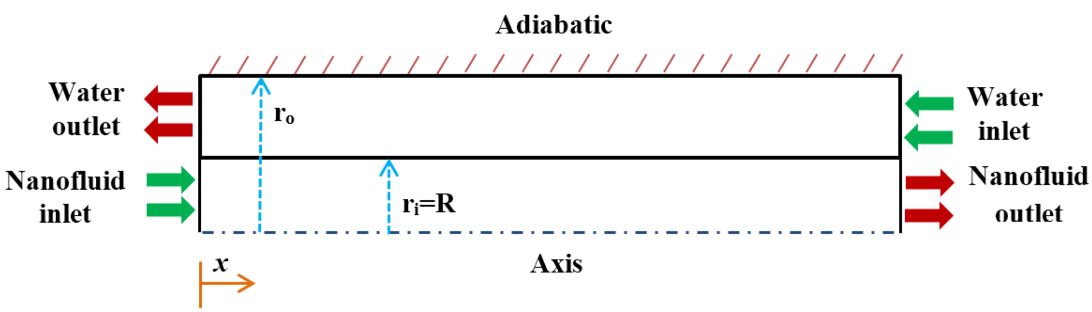

Fig. 3. The mini-channel heat exchanger under study.

6. Results and discussion

In this research, the influences of the shear rate and temperature dependent viscosity and the temperature-dependent thermal conductivity on the hydrothermal characteristics of Fe_3O_4-CNT/water hybrid nanofluid flowing inside a double-pipe heat exchanger are evaluated and compared with those obtained by regarding the hybrid nanofluid as a Newtonian fluid with constant thermal conductivity and viscosity. The simulations are conducted at magnetite concentration range of 0.1-0.9%, CNT concentration range of 0-1.35%, Reynolds number range of 500-2000 for the tube side, and constant Reynolds number of 1000 for the annulus side. The inlet temperature of the nanofluid and water are considered as 298 K and 308 K, respectively. Note that the results of the non-Newtonian and Newtonian Fe_3O_4-CNT/water hybrid nanofluids will be reported by letters 'NN' and 'N', respectively.

Fig. 4 illustrates the variations of viscosity ratio ($\mu_{nf,NN}/\mu_{nf,N}$) for $\varphi_M = 0.7\%$ and $\varphi_{CNT} = 0.7\%$ at three different cross sections (i.e. x=0.1 m, x=0.5 m, and x=0.9 m). For $Re = 500$, by increasing the distance from the tube axis, viscosity of the non-Newtonian hybrid nanofluid diminishes severely at first, and then its descending trend continues at a milder slope, and degree of variations increases with increase in distance from the tube inlet. Near the tube axis, due to small values of shear rate and temperature, viscosity is high. However, by moving away from the tube axis toward the tube wall, both shear rate and temperature increase and consequently, viscosity reduces. The results for $Re = 2000$ indicate that by moving away from the central regions of tube toward the tube wall, viscosity reduces and degree of viscosity variation is lower than that for $Re = 500$. By increasing the Reynolds number at a fixed concentration, the thickness of velocity boundary layer reduces and therefore, the velocity gradient increases. Therefore, there are two reasons for the negligible changes of viscosity in central regions of tube at cross-section x=0.1 m. The first reason is that the shear rate is greater than 60 s^{-1} at most of points of this section, and consequently, fluid viscosity is constant. The second reason is that the thickness of thermal boundary layer in this area is small, which causes constant temperature of the hybrid nanofluid in central regions of tube and thus, viscosity remains unchanged. By moving away from the tube inlet, the thermal boundary layer grows which raises the temperature of the nanofluid in vicinity of the tube wall and, thus, reduces the viscosity. Therefore, the velocity of nanofluid diminishes near the tube wall and increases at the tube axis; i.e. the velocity profile becomes flatter. As a result, the amount of shear rate increases near the tube wall and diminishes near the tube axis; which causes viscosity to diminish near the tube wall and increase near the tube axis. Therefore, it can be said that by moving away from the tube axis, viscosity of the non-Newtonian hybrid nanofluid near the tube wall diminishes; however, its behavior near the tube axis depends on whether the effect of viscosity decrease due to the rise of temperature is greater or the effect of viscosity increase due to the reduction of velocity gradient. Therefore, it is concluded that the effect of temperature increase overcomes the effect of temperature gradient reduction, and viscosity of the non-Newtonian nanofluid diminishes by moving away from the tube inlet. Furthermore, Figs. 4(a) and 4(b) show that viscosity of the non-Newtonian nanofluid diminishes with the increase of Reynolds number. This can be justified based on the reduction of the velocity boundary layer thickness with increasing the Reynolds number, which leads to the increase of velocity gradient and thus the reduction of fluid viscosity. In addition, the comparison between the viscosities of the Newtonian and non-Newtonian hybrid nanofluids indicates that in central regions of the tube, viscosity of the non-Newtonian nanofluid is greater than that of the Newtonian nanofluid; however, in vicinity of the tube wall, the Newtonian fluid has a higher viscosity and by moving away from the tube inlet, the region in which viscosity of the Newtonian nanofluid is greater becomes vaster, since the viscosity of the non-Newtonian nanofluid diminishes by moving away from the tube wall. Both the temperature and shear rate are higher near the tube wall than the tube axis. Therefore, both of these factors lead to the viscosity reduction of the non-Newtonian nanofluids, while the opposite is true near the tube axis.

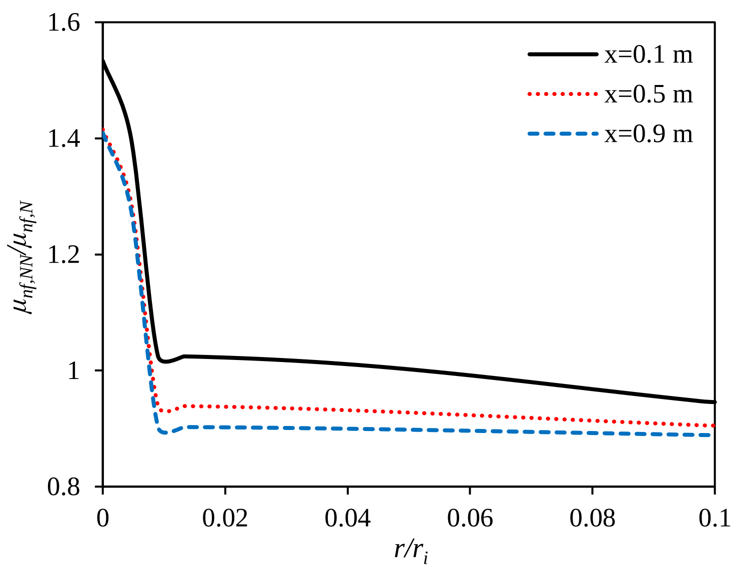

(a)

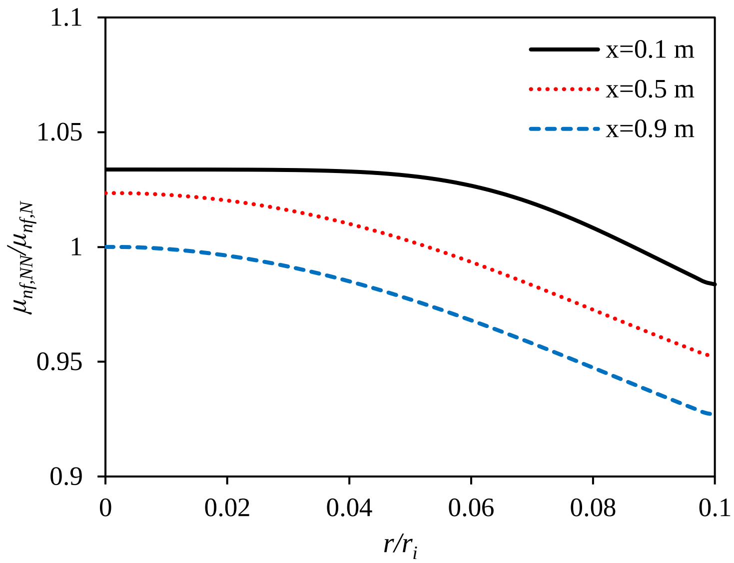

(b)

Fig. 4. Viscosity ratio for $\varphi_M = 0.7\%$ and $\varphi_{CNT} = 0.7\%$ at three different cross sections for (a) $Re = 500$ and (b) $Re = 2000$.

Fig. 5 displays the variations of thermal conductivity ratio ($k_{nf,NN}/k_{nf,N}$) for $\varphi_M = 0.7\%$ and $\varphi_{CNT} = 0.7\%$ at three different cross sections (i.e. x=0.1 m, x=0.5 m, and x=0.9 m). For $Re = 500$, by moving away from the tube axis toward the tube wall, thermal conductivity of the non-Newtonian nanofluid increases continually due to the higher temperature of nanofluid near the wall. The improvement of thermal conductivity with the increase of distance from the tube inlet is due to the higher nanofluid temperature resulting from the increase of heat transfer to the nanofluid. Similar observations exist for $Re = 2000$, with the difference that the slope of thermal conductivity increment near the tube wall is greater for $Re = 2000$. This is due to the rise of nanofluid temperature near the tube wall, resulting from the lower thermal boundary layer thickness that occurs because of the flow velocity enhancement. Moreover, the comparison between thermal conductivity of the Newtonian and non-Newtonian nanofluids shows that thermal conductivity of the non-Newtonian nanofluid is always greater than that of the Newtonian nanofluid; however, the difference between thermal conductivities of the nanofluids reduces with the increase of Reynolds number. Considering the fact that the inlet temperature of nanofluid is 25 ºC, and the thermal conductivity improves with the rise of temperature, it was predictable for the thermal conductivity of non-Newtonian nanofluid to always surpass that for the Newtonian nanofluid. In addition, increasing the Reynolds number reduces the thermal boundary layer thickness and consequently, the internal layers of nanofluid are affected more slowly by wall temperature. This reduces the nanofluid temperature and thereby reduces the thermal conductivity of non-Newtonian nanofluid.

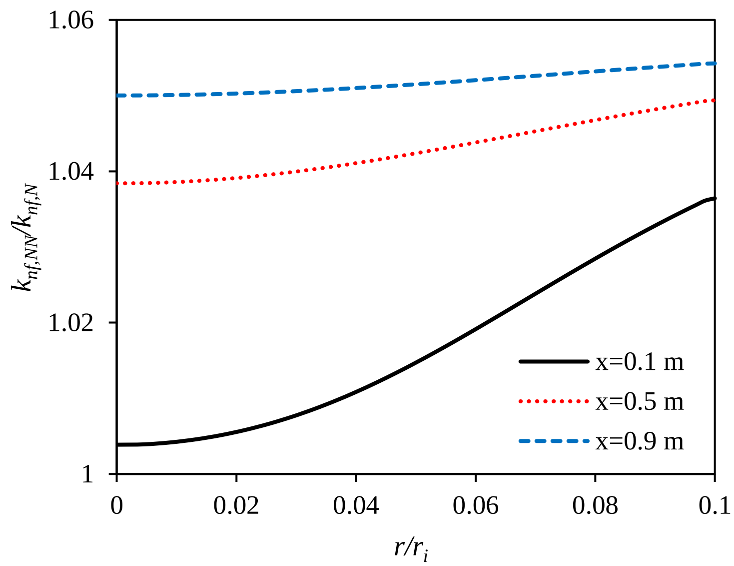

(a)

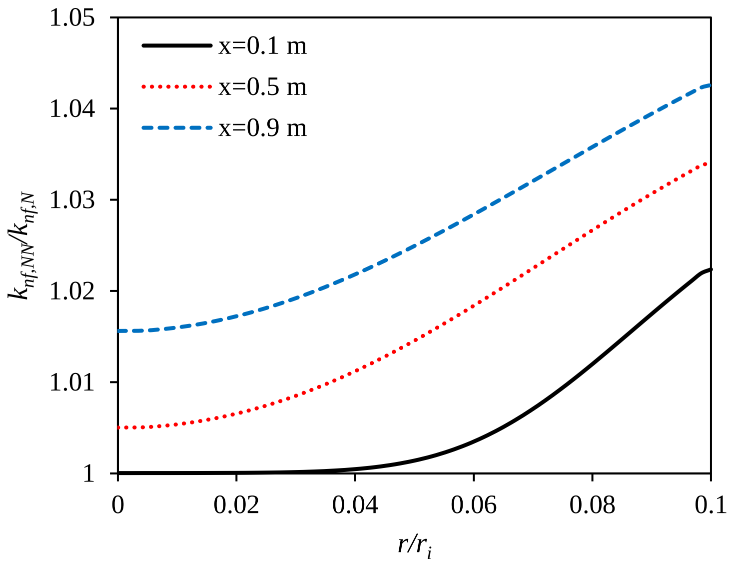

(b)

Fig. 5. Thermal conductivity ratio for $\varphi_M = 0.7\%$ and $\varphi_{CNT} = 0.7\%$ at three different cross sections for (a) $Re = 500$ and (b) $Re = 2000$.

Fig. 6 demonstrates the difference between the pressure drop of the Newtonian and non-Newtonian Fe_3O_4-CNT/water hybrid nanofluids ($d_{\Delta p} = \frac{(\Delta p)_{NN} - (\Delta p)_N}{(\Delta p)_N} \times 100$) in terms of magnetite concentration at different Reynolds numbers. It is seen that the pressure drop of the non-Newtonian nanofluid is always less than that of the Newtonian nanofluid. The minimum pressure drop difference (1.5%) is obtained at $\varphi_M = 0.9\%$, $\varphi_{CNT} = 1.35\%$ and $Re = 2000$, while the maximum difference (9.71%) occurs at $\varphi_M = 0.5\%$, $\varphi_{CNT} = 0.1\%$ and $Re = 500$. Additionally, it is observed that the difference between the pressure drop of the Newtonian and non-Newtonian nanofluids reduces with the increase of Reynolds number. According to Fig. 4, this is caused by the reduction in the difference between the average viscosity of the Newtonian and non-Newtonian nanofluids by increasing the Reynolds number. Furthermore, at $\varphi_{CNT} = 0.1\%$, the pressure drop difference augments when the magnetite concentration increases from 0.1 to 0.3% and then reduces by the further increment of magnetite concentration; while for $\varphi_{CNT} = 1.35\%$, the increase of magnetite concentration results in the reduction in the pressure drop difference. Besides, at $\varphi_M = 0.1\%$, the pressure drop difference rises with increasing the CNT concentration from 0.1 to 1.35%, while the opposite is true at higher magnetite concentrations. According to Darcy's equation ($\Delta p = f \frac{L}{2r_i} \frac{\rho u_{in}^2}{2}$, where f is the friction factor defined as $f = \frac{64}{Re}$ [54]) and by considering the fact that the non-Newtonian and Newtonian nanofluids have the same density and friction factor at an identical Reynolds number, the difference between the pressure drop of the Newtonian and non-Newtonian nanofluids is only due to the difference between their viscosities. It can be concluded from the presented results that the assumption of constant thermal conductivity and viscosity of the hybrid nanofluid, at a low Reynolds number, leads to large errors in the computation of pressure drop; however, the obtained error decreases with the increase of Reynolds number.

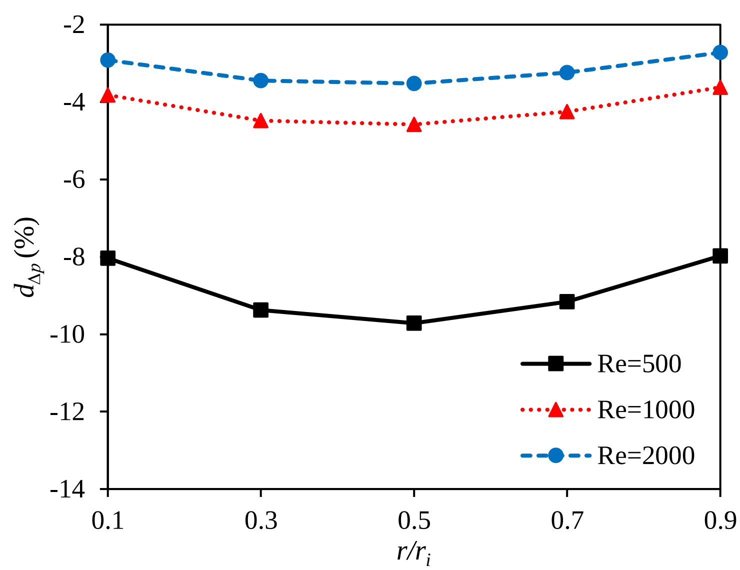

(a)

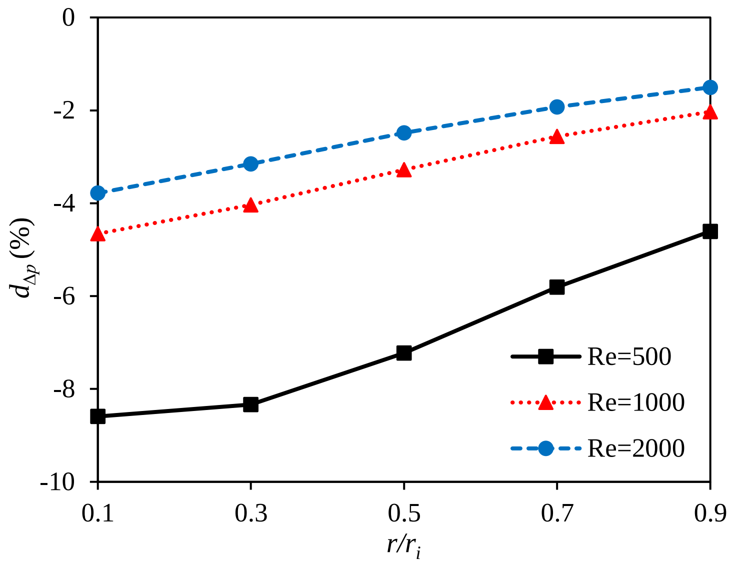

(b)

Fig. 6. Pressure drop at different Reynolds numbers in terms of magnetite concentration at (a) $\varphi_{CNT} = 0.1\%$ and (b) $\varphi_{CNT} = 1.35\%$.

The effects of magnetite concentration on the difference between the heat transfer rate of the Newtonian and non-Newtonian Fe_3O_4-CNT/water hybrid nanofluids ($d_Q = \frac{\dot{Q}_{NN}-\dot{Q}_N}{\dot{Q}_N} \times 100$) at different Reynolds numbers are illustrated in Fig. 7. It is seen that the heat transfer rate of the non-Newtonian hybrid nanofluid is greater than that of the Newtonian nanofluid. The minimum difference (0.31%) is achieved at $\varphi_M = 0.9\%$, $\varphi_{CNT} = 1.35\%$ and $Re = 500$, while the maximum difference (1.23%) occurs at $\varphi_M = 0.1\%$, $\varphi_{CNT} = 1.35\%$ and $Re = 1000$. Additionally, it is observed that with increase in the Reynolds number, the difference between the heat transfer rate of the non-Newtonian and Newtonian nanofluids increases first and then decreases. Increasing the Reynolds number reduces the thermal conductivity and the thermal boundary layer thickness of the non-Newtonian nanofluid, which respectively reduces and increases the rate of heat transfer. In view of Fig. 7, it can be realized that at $Re = 1000$, the effect of reducing the thickness of thermal boundary layer is dominant in comparison with the reduction of thermal conductivity and therefore, the difference between the heat transfer rate of the Newtonian and non-Newtonian nanofluids increases. Meanwhile, for $Re = 2000$, the reduction of thermal conductivity is dominant, which causes a decrease in the difference between the heat transfer rate of the non-Newtonian and Newtonian nanofluids. Moreover, Fig. 7 reveals that at magnetite concentrations of 0.1% and 0.3%, increasing the CNT concentration form 0.1% to 1.35% leads to an increase in the difference between the heat transfer rate of the Newtonian and non-Newtonian nanofluids, whereas the opposite is true for higher magnetite concentrations. Increasing the magnetite concentration leads to the increase of thermal conductivity of the non-Newtonian nanofluid and therefore, the increase of nanofluid outlet temperature, and eventually to the increase of difference between the heat transfer rate of the non-Newtonian and Newtonian nanofluids. Further increase in the magnetite concentration leads to the decrease of the difference between the thermal conductivity of the non-Newtonian and Newtonian nanofluids and therefore, the decrease of the heat transfer rate difference. The results also show that there is no specific pattern on the relationship between the difference in the heat transfer rate of the Newtonian and non-Newtonian nanofluids and the magnetite concentration.

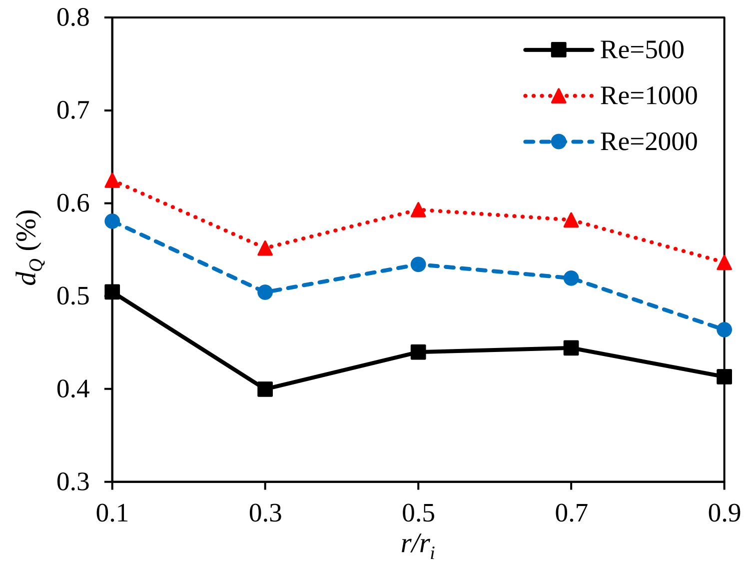

(a)

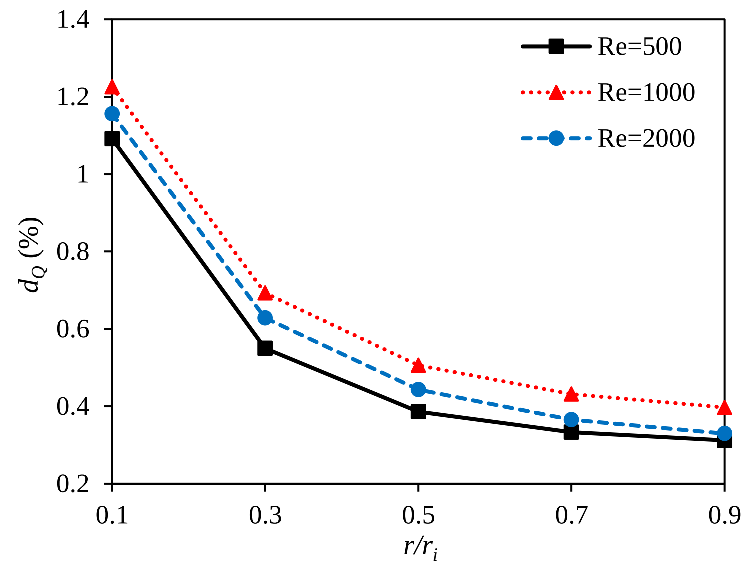

(b)

Fig. 7. Heat transfer rate at different Reynolds numbers in terms of magnetite concentration at (a) $\varphi_{CNT} = 0.1\%$ and (b) $\varphi_{CNT} = 1.35\%$.

Fig. 8 shows the difference between the overall heat transfer coefficient of the Newtonian and non-Newtonian Fe_3O_4-CNT/water hybrid nanofluids ($d_U = \frac{U_{NN} - U_N}{U_N} \times 100$) in terms of magnetite concentration at various Reynolds numbers. It is clear that the overall heat transfer coefficient of the non-Newtonian hybrid nanofluid is greater than that of the Newtonian nanofluid. The minimum difference of the overall heat transfer coefficients (0.58%) is obtained at $\varphi_M = 0.9\%$, $\varphi_{CNT} = 1.35\%$ and $Re = 2000$, while the maximum difference (2.91%) is achieved at $\varphi_M = 0.1\%$, $\varphi_{CNT} = 1.35\%$ and $Re = 500$. Furthermore, the results depicted that the variations of difference between the overall heat transfer coefficient of the Newtonian and non-Newtonian nanofluids with the magnetite and CNT concentrations are similar to that of the difference between the heat transfer rate of these nanofluids. According to the results presented in Fig. 8, it can be concluded that the difference between the overall heat transfer coefficienct of the Newtonian and non-Newtonian nanofluids is less than 3%, which is not significant.

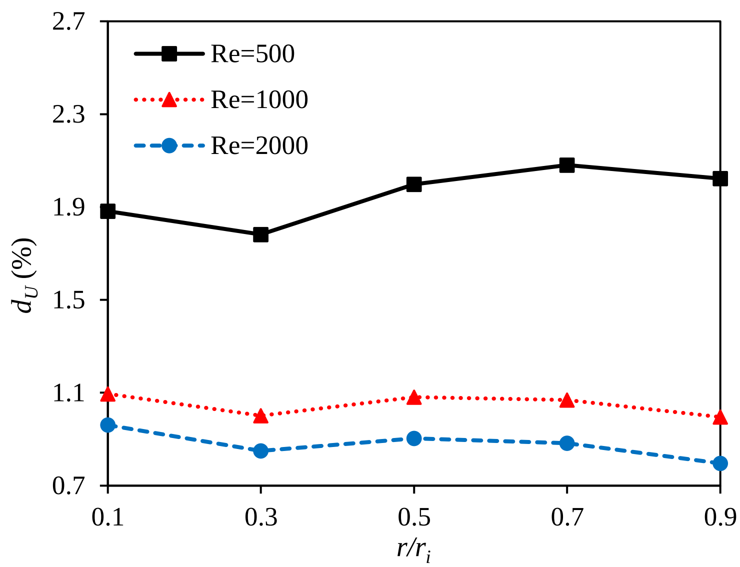

(a)

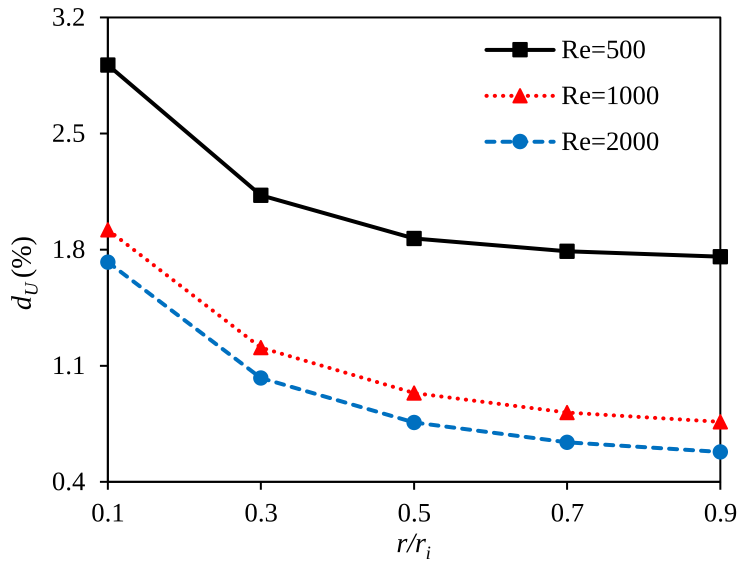

(b)

Fig. 8. Overall heat transfer coefficient at different Reynolds numbers in terms of magnetite concentration at (a) $\varphi_{CNT} = 0.1\%$ and (b) $\varphi_{CNT} = 1.35\%$.

The impacts of magnetite concentration on the difference between the effectiveness of the heat exchangers containing Newtonian and non-Newtonian Fe_3O_4-CNT/water hybrid nanofluids ($d_\varepsilon = \frac{\varepsilon_{NN}-\varepsilon_N}{\varepsilon_N} \times 100$) at different Reynolds numbers are illustrated in Fig. 9. In view of Eq. (12), it can be realized that the trend of effectiveness variations is similar to that of the heat transfer rate variations. Therefore, all the conclusions reached above regarding the heat transfer rate are also true for the effectiveness.

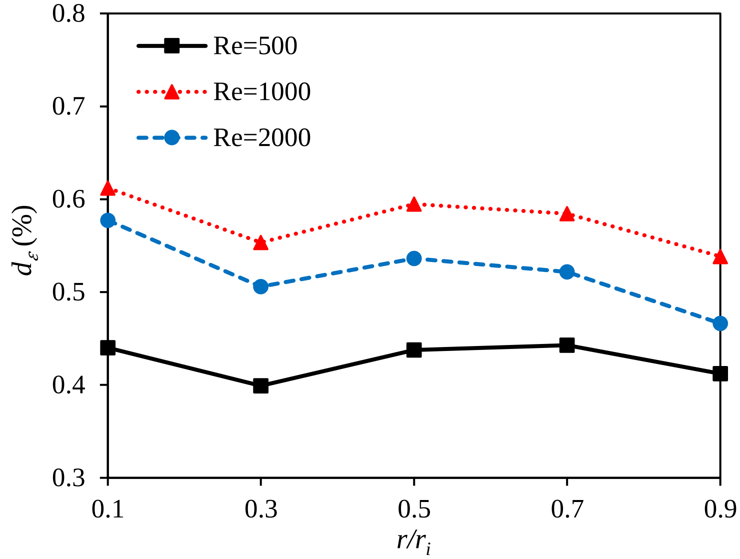

(a)

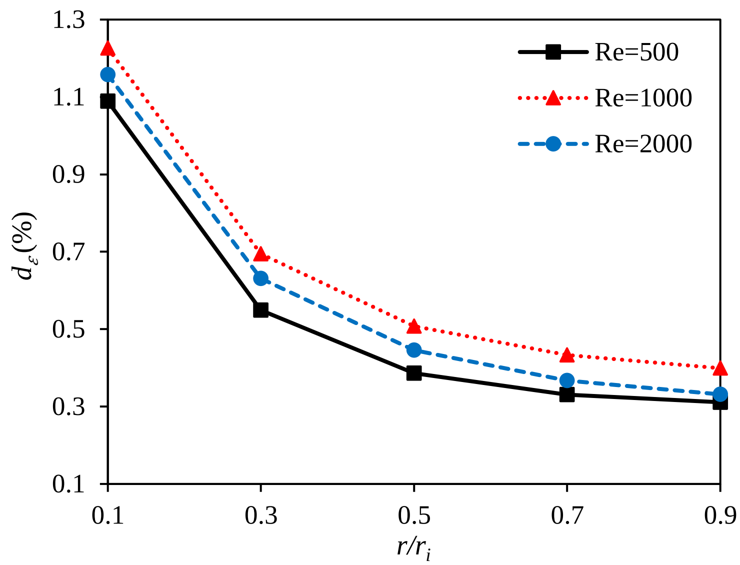

(b)

Fig. 9. Effectiveness of heat exchanger at different Reynolds numbers in terms of magnetite concentration at (a) $\varphi_{CNT} = 0.1\%$ and (b) $\varphi_{CNT} = 1.35\%$.

The pumping power indicates the amount of energy utilized in a heat exchanger. Fig. 10 depicts the difference between the pumping powers of the Newtonian and non-Newtonian Fe_3O_4-

CNT/water hybrid nanofluids ($d_U = \frac{U_{NN} - U_N}{U_N} \times 100$) in terms of magnetite concentration at different Reynolds numbers. It is seen that at a constant Reynolds number, the non-Newtonian hybrid nanofluid always requires less pumping power than the Newtonian nanofluid. The minimum pumping power difference (1.5%) is obtained at $\varphi_M = 0.9\%$, $\varphi_{CNT} = 1.35\%$ and $Re = 2000$, while the maximum difference (9.71%) occurs at $\varphi_M = 0.5\%$, $\varphi_{CNT} = 0.1\%$ and $Re = 500$. In view of Eq. (17), and considering the same average velocity for Newtonian and non-Newtonian nanofluids at similar Reynolds numbers, the difference between the pumping power of the Newtonian and non-Newtonian nanofluids is only related to the difference between their pressure drops. Therefore, at a low Reynolds number, the assumption of constant properties leads to a considerable increase in the pumping power of heat exchangers, whereas the difference reduces with increasing the Reynolds number.

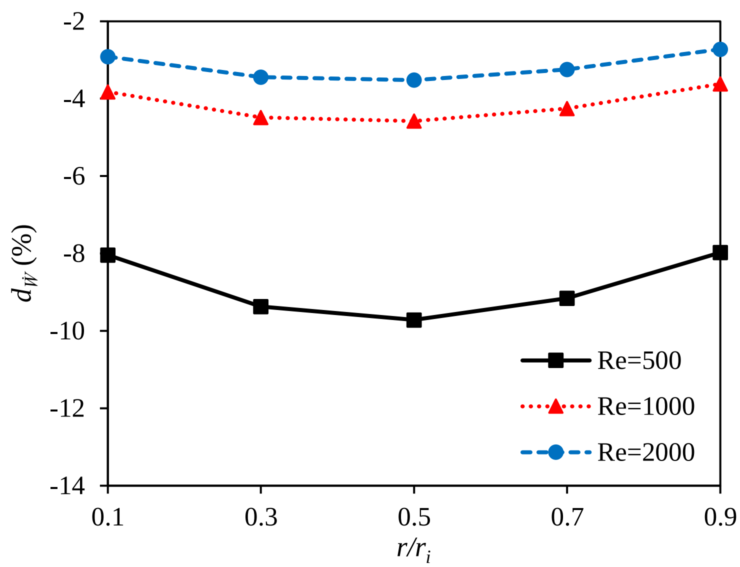

(a)

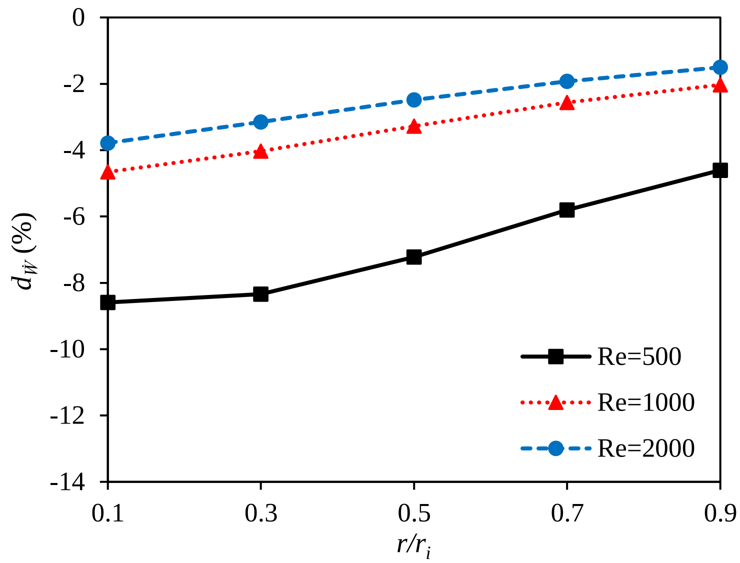

(b)

Fig. 10. Pumping power of heat exchanger at different Reynolds numbers in terms of magnetite concentration at (a) $\varphi_{CNT} = 0.1\%$ and (b) $\varphi_{CNT} = 1.35\%$.

The influences of magnetite concentration on the difference between the performance index of the heat exchangers containing Newtonian and non-Newtonian Fe_3O_4-CNT/water hybrid nanofluids ($d_\varepsilon = \frac{\eta_{NN}-\eta_N}{\eta_N} \times 100$) at different Reynolds numbers are displayed in Fig. 11. It is observed that the heat exchanger containing non-Newtonian nanofluid has a higher performance index than that containing Newtonian nanofluid. The minimum difference (1.86%) is obtained at $\varphi_M = 0.9\%$, $\varphi_{CNT} = 1.35\%$ and $Re = 2000$, while the maximum difference (11.25%) is achieved at $\varphi_M = 0.5\%$, $\varphi_{CNT} = 0.1\%$ and $Re = 500$. Moreover, it is seen that the difference between the performance index of the heat exchangers containing Newtonian and non-Newtonian nanofluids reduces with increase in the Reynolds number. In addition, at $\varphi_{CNT} = 0.1\%$, the performance index difference augments when the magnetite concentration rises from 0.1 to 0.5% and then decreases by the further increment of magnetite concentration; while for $\varphi_{CNT} = 1.35\%$, the increase of magnetite concentration results in the reduction in the performance index difference. Moreover, at $\varphi_M = 0.1\%$, the performance index difference increases with increase in CNT concentration from 0.1 to 1.35%, while the opposite is happen at higher magnetite concentrations. Finally, it can be said that the assumption of constant properties of the Fe_3O_4-CNT/water hybrid nanofluid at low Reynolds numbers and high concentrations of magnetite and CNT nanoparticles, leads to large errors in the computation of performance index of heat exchanger.

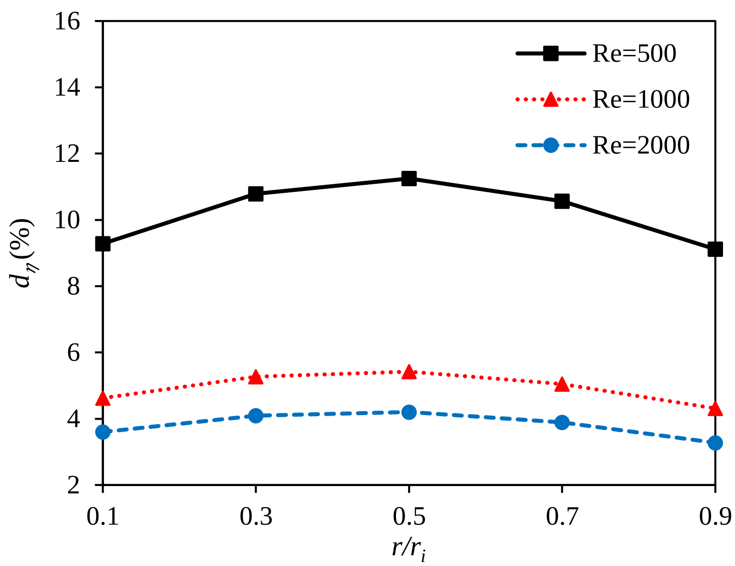

(a)

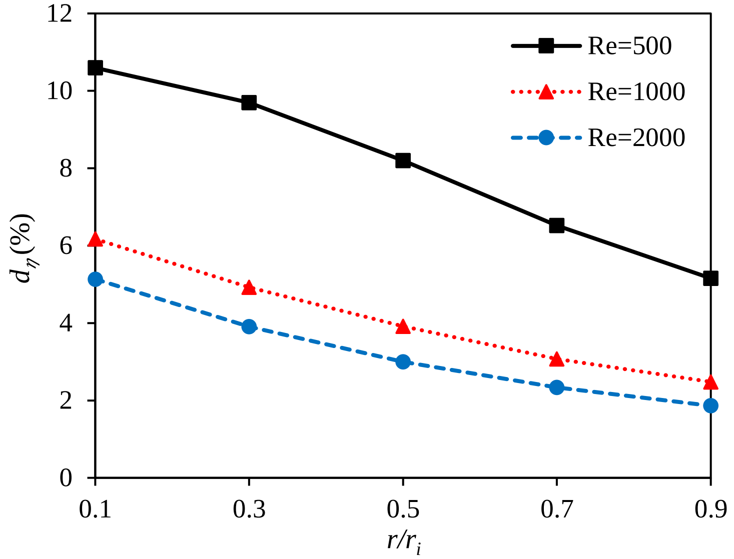

(b)

Fig. 11. Performance index of heat exchanger at different Reynolds numbers in terms of magnetite concentration at (a) $\varphi_{CNT} = 0.1\%$ and (b) $\varphi_{CNT} = 1.35\%$.

7. Conclusion

In this research, the hydrothermal performance of the non-Newtonian Fe_3O_4-CNT/water hybrid nanofluid considering temperature-dependent thermal conductivity and viscosity is numerically evaluated in a double-pipe mini-channel heat exchanger compared with Newtonian Fe_3O_4-CNT/water nanofluid with constant thermal conductivity and viscosity. The comparison is used in order to find how the assumption of constant thermophysical properties of a hybrid nanofluid affects the hydrothermal characteristics in a double-pipe heat exchanger. The obtained results show that in central region of the tube, the non-Newtonian hybrid nanofluid has a higher viscosity compared to the Newtonian nanofluid, while the opposite is true in vicinity of the tube wall. Besides, it is found that the non-Newtonian hybrid nanofluid always has a higher thermal conductivity than the Newtonian nanofluid. In addition, it is seen that the heat transfer rate, overall heat transfer coefficient, effectiveness, and performance index of the non-Newtonian hybrid nanofluid are greater than those of the Newtonian hybrid nanofluid, while the opposite is true for pressure drop and pumping power. The difference between heat transfer rate, overall heat transfer coefficient, effectiveness, and performance index of Newtonian and non-Newtonian hybrid nanofluids augments with increase in the Reynolds number, whereas the difference between the pressure drop and pumping power of nanofluids reduces with increasing the Reynolds number. Furthermore, increment in magnetite and CNT concentrations has no particular effect on the considered parameters. Finally, it can be concluded that by supposing that the Fe_3O_4-CNT/water hybrid nanofluid is a Newtonian fluid with constant thermal conductivity and viscosity, large errors occur in the computation of pressure drop, pumping power, and performance index, whereas the errors in the computation of heat transfer rate, overall heat transfer coefficient, and effectiveness aren't considerable. The results of this study could provide guidelines to better understand the real behaviors of hybrid nanofluids in heat exchangers.

Appendix A

The thermal conductivity correlation:

k_{nf} = 0.22274 tanh (–0.02119T + 0.09807φ_M – 0.06975φ_{CNT} + 0.02528) – 0.67299 tanh (–0.00379T – 0.69125φ_M + 0.11290φ_{CNT} + 0.03221) – 0.26968 tanh (0.12778T + 0.00334φ_M – 0.00362φ_{CNT} + 0.00284) – 0.22184 tanh (0.02121T – 0.09748φ_M + 0.06875φ_{CNT} – 0.02471) – 1.01112 tanh (0.00755T – 0.99285φ_M – 0.05887φ_{CNT} – 0.42417) – 1.04948 tanh (–0.00513T + 0.10775φ_M – 1.43226φ_{CNT} – 0.49474) + 0.51061 tanh (0.00157T – 1.10296φ_M – 1.32512φ_{CNT} + 0.43476) + 0.23038 tanh (–0.02104T + 0.10309φ_M – 0.07821φ_{CNT} + 0.03035) + 0.08974 tanh (0.00333T + 0.05961φ_M + 0.02413φ_{CNT} – 0.03048) + 0.45090 tanh (0.02304T – 0.13733φ_M – 0.48067φ_{CNT} –

$$0.50330) - 0.36153 \tanh(-0.06346T + 0.10622\varphi_M + 0.33903\varphi_{CNT} + 0.29052) - 0.49423 \tanh(-0.00131T + 1.70368\varphi_M - 0.87848\varphi_{CNT} - 0.19465) - 0.21662 \tanh(0.02131T - 0.09401\varphi_M + 0.06297\varphi_{CNT} - 0.02155) - 0.57108 \tanh(-0.00374T - 0.59628\varphi_M + 0.10685\varphi_{CNT} + 0.04961) - 0.27492 \quad \text{(A.1)}$$

The viscosity correlation:

$$\mu_{nf} = -0.24861 \tanh(0.04611\gamma - 0.00068T + 1.06226\varphi_M + 0.13756\varphi_{CNT} + 1.43142) + 1.03130 \tanh(0.47273\gamma + 0.00143T - 0.04534\varphi_M - 0.02812\varphi_{CNT} + 0.40817) - 0.20231 \tanh(-0.17180\gamma + 0.00067T + 1.20978\varphi_M - 0.18044\varphi_{CNT} - 0.25325) - 0.32811 \tanh(0.13316\gamma - 0.00050T - 1.21402\varphi_M + 0.14462\varphi_{CNT} + 0.53138) + 0.30415 \tanh(-0.11840\gamma - 0.00165T + 4.60293\varphi_M - 0.72515\varphi_{CNT} - 3.12857) - 0.00215 \tanh(-0.31607\gamma + 0.00027T - 0.98832\varphi_M + 0.15752\varphi_{CNT} + 4.97709) + 0.41053 \tanh(0.11589\gamma + 0.00148T - 4.37455\varphi_M + 0.62623\varphi_{CNT} + 3.03569) + 0.04707 \tanh(-0.09258\gamma - 0.04017T + 1.06859\varphi_M - 0.09049\varphi_{CNT} - 0.48490) + 0.59719 \tanh(0.04287\gamma + 0.33517T + 1.13670\varphi_M - 0.95007\varphi_{CNT} + 0.04857) + 0.03178 \tanh(-0.02358\gamma - 0.04493T + 0.45525\varphi_M - 0.01014\varphi_{CNT} + 0.45150) + 0.08139 \tanh(-0.09280\gamma + 0.00407T - 1.75844\varphi_M - 0.22328\varphi_{CNT} + 1.44124) - 0.52171 \tanh(0.14031\gamma + 0.00052T - 4.39738\varphi_M - 0.00719\varphi_{CNT} + 3.30400) - 0.04611 \tanh(-0.06569\gamma + 0.00073T + 2.48100\varphi_M + 0.00205\varphi_{CNT} - 1.03603) + 0.08759 \tanh(0.08788\gamma - 0.00410T + 1.69327\varphi_M + 0.22057\varphi_{CNT} - 1.33532) + 0.00066 \tanh(-0.00508\gamma - 0.03150T + 1.26008\varphi_M + 0.43853\varphi_{CNT} + 0.55153) + 0.01716 \tanh(0.14865\gamma - 0.00045T - 0.98651\varphi_M + 0.25307\varphi_{CNT} - 0.85218) + 2.25789 \tanh(-0.06180\gamma + 0.000003T + 2.26987\varphi_M - 0.00222\varphi_{CNT} - 2.86749) - 1.08194 \tanh(-0.11371\gamma - 0.00017T + 3.66682\varphi_M + 0.02690\varphi_{CNT} - 3.01085) + 0.49907 \tanh(-0.48296\gamma - 0.00190T + 0.00935\varphi_M + 0.05003\varphi_{CNT} + 0.09833) - 0.13648 \tanh(-0.02383\gamma - 0.03677T + 0.37656\varphi_M - 0.02106\varphi_{CNT} - 0.42817) + 0.70822 \quad \text{(A.2)}$$

References

[1] Omidi M, Farhadi M, Jafari M. A comprehensive review on double pipe heat exchangers. Applied Thermal Engineering. 2017;110:1075-90.

[2] Ghani S, Gamaledin SMA, Rashwan MM, Atieh MA. Experimental investigation of double-pipe heat exchangers in air conditioning applications. Energy and Buildings. 2018;158:801-11.

[3] Rashidi S, Eskandarian M, Mahian O, Poncet S. Combination of nanofluid and inserts for heat transfer enhancement. Journal of Thermal Analysis and Calorimetry. 2018:1-24.

[4] Izadi M, Behzadmehr A, Shahmardan M. Effects of inclination angle on mixed convection heat transfer of a nanofluid in a square cavity. International Journal for Computational Methods in Engineering Science and Mechanics. 2015;16:11-21.

[5] Pramuanjaroenkij A, Tongkratoke A, Kakaç S. Numerical Study of Mixing Thermal Conductivity Models for Nanofluid Heat Transfer Enhancement. Journal of Engineering Physics and Thermophysics. 2018;91:104-14.

[6] Rashidi S, Karimi N, Mahian O, Esfahani JA. A concise review on the role of nanoparticles upon the productivity of solar desalination systems. Journal of Thermal Analysis and Calorimetry. 2018:1-15.

[7] Mehryan S, Ghalambaz M, Izadi M. Conjugate natural convection of nanofluids inside an enclosure filled by three layers of solid, porous medium and free nanofluid using Buongiorno's and local thermal non-equilibrium models. Journal of Thermal Analysis and Calorimetry.1-21.

[8] Izadi M, Shahmardan M, Maghrebi MJ, Behzadmehr A. Numerical study of developed laminar mixed convection of Al2O3/water nanofluid in an annulus. Chemical Engineering Communications. 2013;200:878-94.

[9] Chol S, Estman J. Enhancing thermal conductivity of fluids with nanoparticles. ASME-Publications-Fed. 1995;231:99-106.

[10] Rashidi S, Mahian O, Languri EM. Applications of nanofluids in condensing and evaporating systems. Journal of Thermal Analysis and Calorimetry. 2018;131:2027-39.

[11] Rashidi S, Javadi P, Esfahani JA. Second law of thermodynamics analysis for nanofluid turbulent flow inside a solar heater with the ribbed absorber plate. Journal of Thermal Analysis and Calorimetry. 2018:1-13.

[12] Akbarzadeh M, Rashidi S, Karimi N, Omar N. First and second laws of thermodynamics analysis of nanofluid flow inside a heat exchanger duct with wavy walls and a porous insert. Journal of Thermal Analysis and Calorimetry. 2018:1-18.

[13] Rashidi S, Akbarzadeh M, Karimi N, Masoodi R. Combined effects of nanofluid and transverse twisted-baffles on the flow structures, heat transfer and irreversibilities inside a square duct–a numerical study. Applied Thermal Engineering. 2018;130:135-48.

[14] Shamsabadi H, Rashidi S, Esfahani JA. Entropy generation analysis for nanofluid flow inside a duct equipped with porous baffles. Journal of Thermal Analysis and Calorimetry.1-11.

[15] Izadi M, Sinaei S, Mehryan S, Oztop HF, Abu-Hamdeh N. Natural convection of a nanofluid between two eccentric cylinders saturated by porous material: Buongiorno's two phase model. International Journal of Heat and Mass Transfer. 2018;127:67-75.

[16] Izadi M, Shahmardan M, Norouzi M, Rashidi A, Behzadmehr A. Cooling performance of a nanofluid flow in a heat sink microchannel with axial conduction effect. Applied Physics A. 2014;117:1821-33.

[17] Izadi M, Behzadmehr A, Shahmardan MM. Effects of discrete source-sink arrangements on mixed convection in a square cavity filled by nanofluid. Korean Journal of Chemical Engineering. 2014;31:12-9.

[18] Shakiba A, Vahedi K. Numerical analysis of magnetic field effects on hydro-thermal behavior of a magnetic nanofluid in a double pipe heat exchanger. Journal of Magnetism and Magnetic Materials. 2016;402:131-42.

[19] Azmi WH, Sharma KV, Mamat R, Najafi G, Mohamad MS. The enhancement of effective thermal conductivity and effective dynamic viscosity of nanofluids – A review. Renewable and Sustainable Energy Reviews. 2016;53:1046-58.

[20] Toghraie D, Chaharsoghi VA, Afrand M. Measurement of thermal conductivity of ZnO–TiO2/EG hybrid nanofluid. Journal of Thermal Analysis and Calorimetry. 2016;125:527-35.

[21] Pryazhnikov MI, Minakov AV, Rudyak VY, Guzei DV. Thermal conductivity measurements of nanofluids. International Journal of Heat and Mass Transfer. 2017;104:1275-82.

[22] Alirezaie A, Hajmohammad MH, Hassani Ahangar MR, Hemmat Esfe M. Price-performance evaluation of thermal conductivity enhancement of nanofluids with different particle sizes. Applied Thermal Engineering. 2018;128:373-80.

[23] Maddah H, Alizadeh M, Ghasemi N, Alwi SRW. Experimental study of Al2O3/water nanofluid turbulent heat transfer enhancement in the horizontal double pipes fitted with modified twisted tapes. International Journal of Heat and Mass Transfer. 2014;78:1042-54.

[24] Mousavi SV, Sheikholeslami M, Gerdroodbary MB. The Influence of magnetic field on heat transfer of magnetic nanofluid in a sinusoidal double pipe heat exchanger. Chemical Engineering Research and Design. 2016;113:112-24.

[25] Saeedan M, Nazar ARS, Abbasi Y, Karimi R. CFD Investigation and neutral network modeling of heat transfer and pressure drop of nanofluids in double pipe helically baffled heat exchanger with a 3-D fined tube. Applied Thermal Engineering. 2016;100:721-9.

[26] Sarafraz M, Hormozi F, Nikkhah V. Thermal performance of a counter-current double pipe heat exchanger working with COOH-CNT/water nanofluids. Experimental Thermal and Fluid Science. 2016;78:41-9.

[27] Kumar NR, Bhramara P, Sundar LS, Singh MK, Sousa AC. Heat transfer, friction factor and effectiveness of Fe3O4 nanofluid flow in an inner tube of double pipe U-bend heat exchanger with and without longitudinal strip inserts. Experimental Thermal and Fluid Science. 2017;85:331-43.

[28] Hussein AM. Thermal performance and thermal properties of hybrid nanofluid laminar flow in a double pipe heat exchanger. Experimental Thermal and Fluid Science. 2017;88:37-45.

[29] Shirvan KM, Mamourian M, Mirzakhanlari S, Ellahi R. Numerical investigation of heat exchanger effectiveness in a double pipe heat exchanger filled with nanofluid: a sensitivity analysis by response surface methodology. Powder Technology. 2017;313:99-111.

[30] Afrand M, Toghraie D, Ruhani B. Effects of temperature and nanoparticles concentration on rheological behavior of Fe3O4–Ag/EG hybrid nanofluid: an experimental study. Experimental Thermal and Fluid Science. 2016;77:38-44.

[31] Rostamian SH, Biglari M, Saedodin S, Esfe MH. An inspection of thermal conductivity of CuO-SWCNTs hybrid nanofluid versus temperature and concentration using experimental data, ANN modeling and new correlation. Journal of Molecular Liquids. 2017;231:364-9.

[32] Esfe MH, Alirezaie A, Rejvani M. An applicable study on the thermal conductivity of SWCNT-MgO hybrid nanofluid and price-performance analysis for energy management. Applied Thermal Engineering. 2017;111:1202-10.

[33] Esfahani NN, Toghraie D, Afrand M. A new correlation for predicting the thermal conductivity of ZnO–Ag (50%–50%)/water hybrid nanofluid: An experimental study. Powder Technology. 2018;323:367-73.

[34] Moldoveanu GM, Huminic G, Minea AA, Huminic A. Experimental study on thermal conductivity of stabilized Al2O3 and SiO2 nanofluids and their hybrid. International Journal of Heat and Mass Transfer. 2018;127:450-7.

[35] Karimi A, Afrand M. Numerical study on thermal performance of an air-cooled heat exchanger: Effects of hybrid nanofluid, pipe arrangement and cross section. Energy Conversion and Management. 2018;164:615-28.

[36] Izadi M, Mohebbi R, Karimi D, Sheremet MA. Numerical simulation of natural convection heat transfer inside a⊥ shaped cavity filled by a MWCNT-Fe3O4/water hybrid nanofluids using LBM. Chemical Engineering and Processing-Process Intensification. 2018;125:56-66.

[37] Esfe MH, Esfandeh S, Afrand M, Rejvani M, Rostamian SH. Experimental evaluation, new correlation proposing and ANN modeling of thermal properties of EG based hybrid nanofluid containing ZnO-DWCNT nanoparticles for internal combustion engines applications. Applied Thermal Engineering. 2018;133:452-63.

[38] Theres Baby T, Sundara R. Surfactant free magnetic nanofluids based on core-shell type nanoparticle decorated multiwalled carbon nanotubes. Journal of Applied Physics. 2011;110:064325.

[39] Felicia LJ, Philip J. Magnetorheological properties of a magnetic nanofluid with dispersed carbon nanotubes. Physical Review E. 2014;89:022310.

[40] Sundar LS, Singh MK, Sousa AC. Enhanced heat transfer and friction factor of MWCNT–Fe3O4/water hybrid nanofluids. International Communications in Heat and Mass Transfer. 2014;52:73-83.

[41] Shahsavar A, Saghafian M, Salimpour M, Shafii M. Experimental investigation on laminar forced convective heat transfer of ferrofluid loaded with carbon nanotubes under constant and alternating magnetic fields. Experimental Thermal and Fluid Science. 2016;76:1-11.

[42] Harandi SS, Karimipour A, Afrand M, Akbari M, D'Orazio A. An experimental study on thermal conductivity of F-MWCNTs–Fe3O4/EG hybrid nanofluid: effects of temperature and concentration. International Communications in Heat and Mass Transfer. 2016;76:171-7.

[43] Moradi H, Bazooyar B, Etemad SG, Moheb A. Influence of the geometry of cylindrical enclosure on natural convection heat transfer of Newtonian nanofluids. Chemical Engineering Research and Design. 2015;94:673-80.

[44] Hojjat M. Modeling heat transfer of non-Newtonian nanofluids using hybrid ANN-Metaheuristic optimization algorithm. Journal of Particle Science & Technology. 2018;3:233-41.

[45] Sandeep N, Malvandi A. Enhanced heat transfer in liquid thin film flow of non-Newtonian nanofluids embedded with graphene nanoparticles. Advanced Powder Technology. 2016;27:2448-56.

[46] Akbari OA, Toghraie D, Karimipour A, Marzban A, Ahmadi GR. The effect of velocity and dimension of solid nanoparticles on heat transfer in non-Newtonian nanofluid. Physica E: Low-dimensional Systems and Nanostructures. 2017;86:68-75.

[47] Singh AK, Kishore N. Laminar Mixed Convection of Non-Newtonian Nanofluids Flowing Vertically Upward Across a Confined Circular Cylinder. Journal of Thermal Science and Engineering Applications. 2018;10:041012--14.

[48] Shahsavar A, Saghafian M, Salimpour M, Shafii M. Effect of temperature and concentration on thermal conductivity and viscosity of ferrofluid loaded with carbon nanotubes. Heat and Mass Transfer. 2016;52:2293-301.

[49] Berger P, Adelman NB, Beckman KJ, Campbell DJ, Ellis AB, Lisensky GC. Preparation and properties of an aqueous ferrofluid. Journal of Chemical Education. 1999;76:943.

[50] Garg P, Alvarado JL, Marsh C, Carlson TA, Kessler DA, Annamalai K. An experimental study on the effect of ultrasonication on viscosity and heat transfer performance of multi-wall carbon nanotube-based aqueous nanofluids. International Journal of Heat and Mass Transfer. 2009;52:5090-101.

[51] Shahsavar A, Bahiraei M. Experimental investigation and modeling of thermal conductivity and viscosity for non-Newtonian hybrid nanofluid containing coated CNT/Fe3O4 nanoparticles. Powder Technology. 2017;318:441-50.

[52] Mohammed HA, Narrein K. Thermal and hydraulic characteristics of nanofluid flow in a helically coiled tube heat exchanger. International Communications in Heat and Mass Transfer. 2012;39:1375-83.

[53] Duangthongsuk W, Wongwises S. An experimental study on the heat transfer performance and pressure drop of TiO2-water nanofluids flowing under a turbulent flow regime. International Journal of Heat and Mass Transfer. 2010;53:334-44.

[54] Lienhard JH. A heat transfer textbook: Courier Corporation; 2013.